ACS APPLIED MATERIALS & INTERFACES

Research Article

www.acsami.org

Design of Thermally Responsive Polymeric Hydrogels for Brackish Water Desalination: Effect of Architecture on Swelling, Deswelling, and Salt Rejection

Wael Ali,[†] Beate Gebert,[‡] Tobias Hennecke,[§] Karlheinz Graf,[†,⊥] Mathias Ulbricht,[§] and Jochen S. Gutmann*[,†,‡]

[†]Physikalische Chemie and CENIDE (Center for Nanointegration), Universität Duisburg-Essen, Universitätsstrasse 2, 45141 Essen, Germany

[‡]Deutsches Textilforschungszentrum Nord-West e. V., Adlerstrasse 1, 47798 Krefeld, Germany

[§]Technische Chemie II and CENIDE (Center for Nanointegration), Universität Duisburg-Essen, Universitätsstrasse 5, 45141 Essen, Germany

[⊥]Physikalische Chemie, Hochschule Niederrhein, Adlerstrasse 32, 47798 Krefeld, Germany

Supporting Information

ABSTRACT: In this work, we explore the ability of utilizing hydrogels synthesized from a temperature-sensitive polymer and a polyelectrolyte to desalinate salt water by means of reversible thermally induced absorption and desorption. Thus, the influence of the macromolecular architecture on the swelling/deswelling behavior for such hydrogels was investigated by tailor-made network structures. To this end, a series of chemically cross-linked polymeric hydrogels were synthesized via free radical-initiated copolymerization of sodium acrylate (SA) with the thermoresponsive comonomer *N*-isopropylacrylamide (NIPAAm) by realizing different structural types. In particular, two different polyNIPAAm macromonomers, either with one acrylate function at the chain end or with additional acrylate functions as side groups were synthesized by controlled polymerization and subsequent polymer-analogous reaction and then used as building blocks. The rheological behaviors of hydrogels and their estimated mesh sizes are discussed. The performance of the hydrogels in terms of swelling and deswelling in both deionized water (DI) and brackish water (2 g/L NaCl) was measured as a function of cross-linking degree and particle size. The salt content could be reduced by 23% in one cycle by using the best performing material.

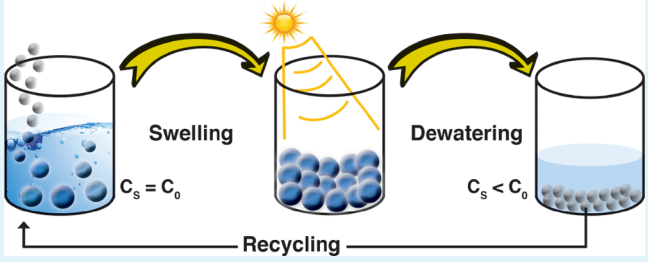

KEYWORDS: *desalination, thermally responsive hydrogel, polyelectrolyte hydrogel, macromolecular architecture, N-isopropylacrylamide, sodium acrylate*

INTRODUCTION

It has been widely recognized that the depletion of fresh, potable water poses one of the major challenges for our society. Currently, the water use is growing twice as rapidly as population, and over the next 25 years, the number of people worldwide affected by severe water shortages is expected to increase 4-fold if current consumption continues.[1,2] In addition, even modern economies cannot develop and thrive without sufficient access to water and without sustainable global energy supply. In contrast, brackish water and seawater could easily satisfy human water needs with appropriate desalination.[3] Current technology,[4] which is mostly dominated by reverse osmosis (RO) and multistage flash (MSF) evaporation, are energy-intensive processes due to high osmotic pressure of seawater and limited energy efficiency of conventional thermal separation.[5] Thus, developing low cost technologies or methods for water purification and seawater desalination are of strategic importance for meeting the current and future needs for water. The present work relates to a method for the desalination of nonpotable brackish water to make it useful for human consumption by reversible thermally induced swelling and deswelling of a special class of polymeric hydrogels.

Hydrogels are cross-linked, three-dimensional hydrophilic polymer networks, which swell but do not dissolve when brought into contact with water.[6] In particular, a cross-linked polyelectrolyte is able to entrap large volumes of water because of the osmotic pressure difference between the interior of the hydrogel and the surrounding solution.[7,8] Polyelectrolyte hydrogel based on a weakly cross-linked poly(acrylic acid)/poly(sodium acrylate) copolymer with polymer volume fractions between 0.03 and 0.3 exhibit swelling pressure in the range of 0.20−4.23 MPa.[9] Such hydrogels with higher

Received: October 6, 2014
Accepted: June 19, 2015
Published: June 19, 2015

DOI: 10.1021/acsami.5b03878
ACS Appl. Mater. Interfaces 2015, 7, 15696−15706

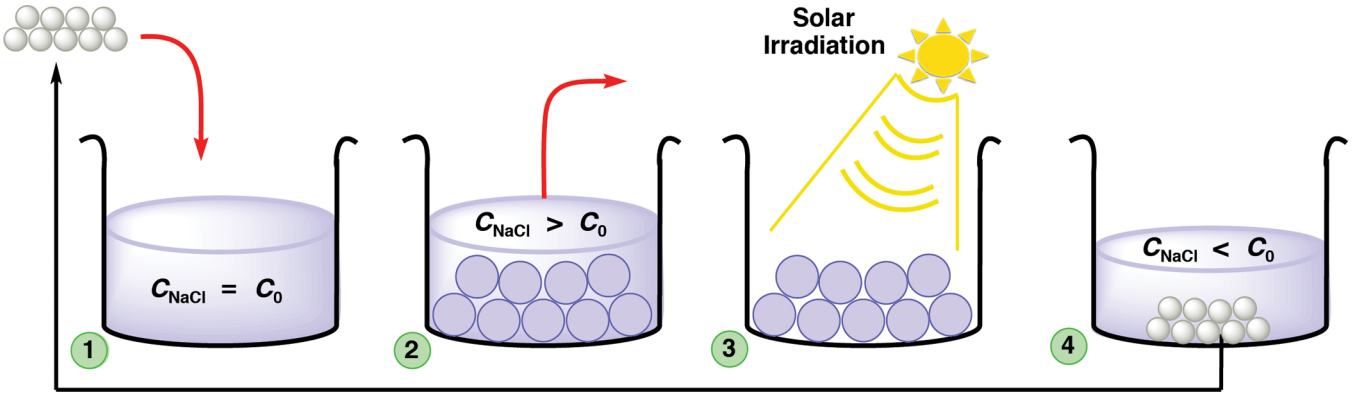

Figure 1. Schematic representation of the envisioned four steps of the desalination process: (1) swelling of the hydrogel in an excess of salt water, (2) removal of the excess solution, (3) dewatering of the hydrogel by means of thermal energy source, and (4) acquisition of salt depleted water and hydrogel recycling.

Scheme 1. Synthesis of Polymeric Hydrogel Entities Using Polyelectrolyte and Different Types of a Thermoresponsive Comonomer As Indicated in the Suggested Network Structures

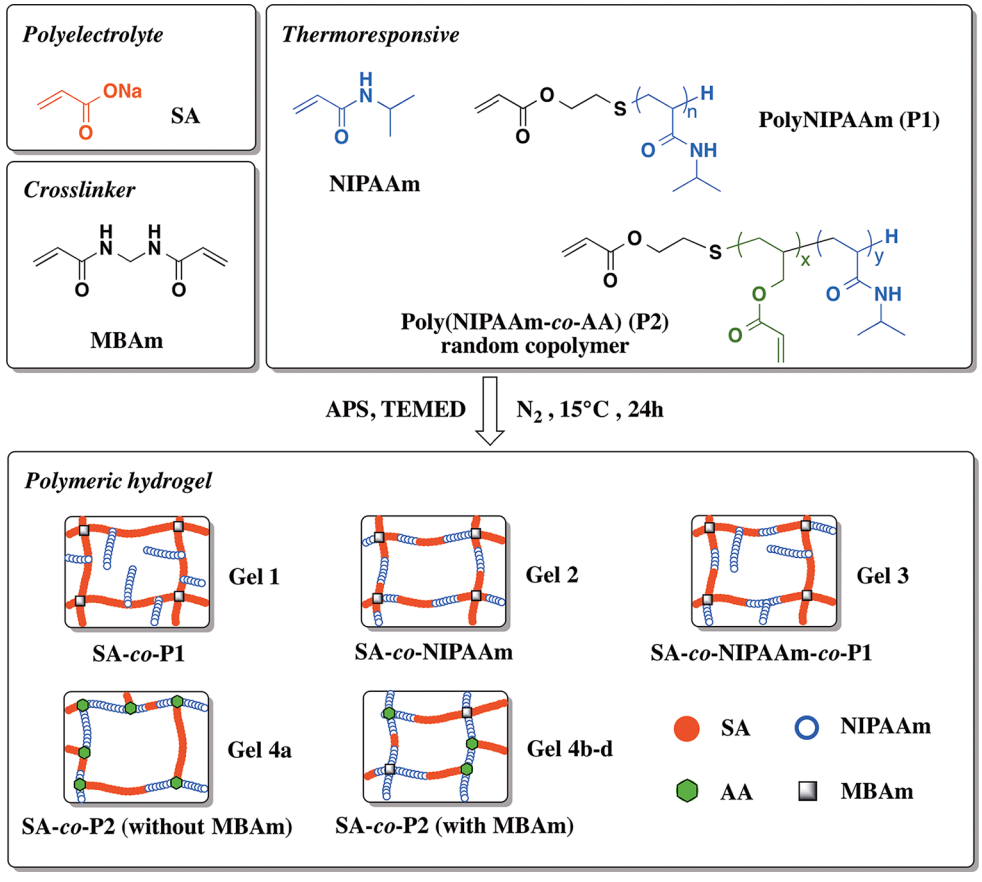

polymer fraction in contact with seawater (typical salt concentration: 35 g/L) will take up preferably salt depleted water since the osmotic pressure of seawater is 2.34 MPa at 25 °C. According to this fact, Wilhelm et al. have recently developed a new approach for the desalination of seawater by free swelling and mechanical deswelling polyacrylic hydrogels and as a result of their principle the salt content could be reduced by 35% in one cycle for a 10 g/L NaCl feed solution.[10]

One of the most remarkable areas that have attracted much attention in the field of hydrogel science is their stimulus sensitivity. Hydrogels composed of stimuli-responsive polymers, which are also known as "smart" or "intelligent" hydrogels, undergo abrupt reversible changes in volume or shape upon application of external stimuli,[11,12] such as temperature, pH, ionic strength, specific ions or molecules, electric field, magnetic field, and light. Among them, temperature-responsive hydrogels are most commonly used due to the facile tuning of their properties. Particularly, poly(*N*-isopropylacrylamide) (polyNIPAAm) is a typical thermosensitive polymeric material that demonstrates a transition temperature or lower critical solution temperature (LCST) at around 32 °C in aqueous solution.[13,14] Thus, hydrogels composed of polyNIPAAm undergo reversibly phase separation as the external temperature cycles around the LCST. The thermo-

DOI: 10.1021/acsami.5b03878
ACS Appl. Mater. Interfaces 2015, 7, 15696−15706

Table 1. Feed Composition and Monomer Conversions for the Hydrogels Used within This Study

sample	code	feed composition (wt %) SA	NIPAAm	P1	P2	MBAm[a]	conversion[b] (wt %)
PNIPAAm	PNIPAAm gel		100			7	98
PSA-*co*-P1 (DC07)	Gel 1	50	0	50		7	94
PSA-*co*-PNIPAAm (DC03)	Gel 2a	50	50			2	96
PSA-*co*-PNIPAAm (DC05)	Gel 2b	50	50			5	97
PSA-*co*-PNIPAAm (DC07)	Gel 2c	50	50			7	97
PSA-*co*-PNIPAAm-*co*-P1 (DC07)	Gel 3	50	25	25		7	96
PSA-*co*-P2 (DC04)	Gel 4a	50			50		98
PSA-*co*-P2 (DC07)	Gel 4b	50			50	2	97
PSA-*co*-P2 (DC09)	Gel 4c	50			50	5	98
PSA-*co*-P2 (DC011)	Gel 4d	50			50	7	97

[a]Relative to total monomer concentration. [b]Weight percent of synthesized dry hydrogel to the monomers.

reversible property of phase separation has a variety of applications in many fields, including solute extraction and separation, controlled drug delivery, actuators, sensors, and enzyme immobilization.[15,16] By combination of the two types of hydrogels mentioned above, it might be possible to reduce the salinity of water such as brackish water as illustrated schematically in Figure 1.

Actually, several expired patents that are related to a similar desalination process have been reported using poly(vinyl alcohol) acetate and ethoxylated cellulose resins,[17] cross-linked polyurethanes,[18] a polymer from *N*-vinyl-2-ethyl imidazole cross-linked with α,α'-dibromo-*p*-xylene,[19] phosphorus containing polyolefins,[20] acrylate/acrylic acid copolymer,[21] and polyurethanes wherein the polyol is a triblock copolymer (Pluronics).[22] The release of water for all these types of absorbents has been achieved by heating up the water and the immersed absorbent. In a similar manner Wang et al. have recently demonstrated the utilization of stimuli-responsive polymer hydrogels as a draw agent for forward osmosis desalination and solar dewatering by simple exposure to simulated sunlight.[23] Furthermore, they have also shown that the swelling property of these hydrogels and the water recovery rate can be dramatically increased via the incorporation of hydrophilic carbon particles or reduced graphene oxide (rGO).[24,25] The same group has recently demonstrated the utility of composite hydrogel in the presence of magnetic nanoparticles to enhance the liquid water recovery (to 53%) under magnetically induced heating.[26] Nevertheless, the efficiency of this technology is still far away from application. In order to achieve high efficiency for such desalination process, hydrogels should be designed to meet the following requirements: (i) high salt expelling ability (high osmotic pressure), (ii) excellent water uptake, (iii) fast thermoresponsivity for the absorption−desorption operating system, (iv) hydrogel recycling ability at low energy cost.

In this paper, we will discuss the effect of the macromolecular architecture on the swelling/deswelling behavior of stimuli-responsive hydrogels in salt solution by tailoring the gel architecture at the molecular level. Thus, a series of chemically cross-linked polymeric hydrogels was synthesized via free radical-initiated copolymerization of sodium acrylate (SA) with various structural types of the thermoresponsive comonomer *N*-isopropylacrylamide (NIPAAm) as depicted in Scheme 1. To this end, we first synthesized alcohol-terminated polyNIPAAm and poly(*N*-isopropylacrylamide-*co*-allyl alcohol) random copolymer (poly(NIPAAm-*co*-AAL)). Thereafter, a polymerizable acrylate group was introduced into the polymers via a condensation reaction to obtain polyNIPAAm (P1) as macromonomer and poly(*N*-isopropylacrylamide-*co*-allyl acrylate) (poly(NIPAAm-*co*-AA)) (P2) as macromonomer and cross-linking agent at the same time. Introducing a comb-type polyNIPAAm grafted chain to the gel network is advantageous to their ability to exhibit a rapid response in terms of dewatering. In previous works, other groups have shown that the freely mobile polyNIPAAm grafted chains readily caused hydrophobic aggregation and subsequently triggered dehydration of the whole network.[27−29]

EXPERIMENTAL SECTION

Materials. *N*-Isopropylacrylamide (NIPAAm, 99%, Sigma-Aldrich) was purified by recrystallization in hexane and dried in vacuo. 2,2′-Azobis(isobutyronitrile) (AIBN, 98%, Sigma-Aldrich) was recrystallized from ethanol twice before use. Sodium acrylate (SA) (99%), *N*,*N*′-methylenbis(acrylamide) (MBAm) (99%), 2-hydroxyethanethiol (HESH) (99%), *N*,*N*,*N*′,*N*′-tetramethylethylenediamine (TEMED) (99.5%), allyl alcohol (AAL) (99%), and acryloyl chloride (AC) (97%) were all purchased from Sigma-Aldrich and used as received. Ammonium persulfate (APS) (99.5%), sodium chloride (99.5%), and potassium chloride (99%) were all obtained from Acros Organics, Geel, Belgium. The solvents such as tetrahydrofuran (THF), chloroform, acetone, and diethyl ether were obtained from commercial sources. Before use, THF was purified using aluminum oxide 90 basic. The water used throughout this study was deionized water from a Milli-Q system (Millipore).

Synthesis of polyNIPAAm Macromonomer (P1). The polyNIPAAm macromonomer was prepared as follows: First, a semitelechelic polyNIPAAm with a terminal hydroxyl end group polyNIPAAm−OH was synthesized by radical telomerization of the NIPAAm monomer utilizing HESH as a chain transfer agent. Typically, NIPAAm (5.65 g, 50 mmol), HESH (0.316 g, 4 mmol), and AIBN (0.084 g, 0.5 mmol) as an initiator were charged to a three-necked flask with a magnetic stirrer and dissolved in THF (20 mL). The monomer solution was degassed by a freeze−thaw cycle and sealed in vacuum. Polymerization was carried out for 15 h at 70 °C under nitrogen atmosphere. After concentrating the reactant by THF evaporation, the reactant was poured into diethyl ether to precipitate polyNIPAAm−OH. PolyNIPAAm−OH was collected by filtration and purified by repeated precipitation in diethyl ether from acetone. The polymer was isolated by freeze-drying from aqueous solution. For the second step, the purified polyNIPAAm−OH was dissolved in chloroform and acryloyl chloride (excess) was instilled. The reaction mixture was stirred at 40 °C for 2 h under a nitrogen atmosphere. The purification process for polyNIPAAm macromonomer followed the same process as for polyNIPAAm−OH.

Synthesis of Poly(NIPAAm-*co*-AA) Macromonomer (P2). Poly(NIPAAm-*co*-AA) cross-linker macromonomer was prepared according to the same procedure described above for polyNIPAAm

DOI: 10.1021/acsami.5b03878
ACS Appl. Mater. Interfaces 2015, 7, 15696−15706

macromonomer (P1) using 10 wt % AAL as a comonomer with respect to NIPAAm monomer.

Synthesis of Hydrogels. To synthesize the hydrogels depicted in Scheme 1, we dissolved 10 wt % monomers solution of sodium acrylate (SA), thermosensitive comonomer or macromonomer, and MBAm as cross-linker in 10 mL of water in a glass vial (25 mm in diameter). The monomers solution was stirred and nitrogen gas was bubbled under cooling (4 °C) over a period of 20 min to remove residual oxygen. Afterward, 8 mg of APS (0.5 wt % with respect to monomers) as an initiator and 42 μL of TEMED (mass ratio of TEMED to APS; 4:1) as an accelerator were added, respectively. The reaction mixture was immediately poured into a double-jacketed glass vessel (70 mm in diameter). The vessel was sealed, and the radical polymerization was carried out for 24 h at 15 °C under nitrogen atmosphere. The obtained hydrogels were cut into discs (13 mm in diameter and 3 mm in thickness), immersed in distilled water at room temperature with water being daily refreshed to remove unreacted materials and allowing equilibrium swelling. The polyNIPAAm hydrogel (PNIPAAm gel) was also prepared and purified by the same method. A comprehensive account on the samples used and their respective composition as well as the degree of monomer conversion is given in Table 1.

Characterization and Measurements. *Scanning Electron Microscopy (SEM).* SEM images of dried hydrogels were recorded with a SEM S-3400 N II of Hitachi High-Technologies Europe GmbH. The hydrogel disks were first immersed in deionized water at room temperature (~23 °C) up to swelling at equilibrium and subsequently frozen at −196 °C by dipping in liquid nitrogen. The frozen samples were fractured and freeze-dried at −50 °C for 24 h using the Christ Alpha 1−4 freeze-dryer.

Nuclear Magnetic Resonance Spectroscopy (NMR). ^{1}H NMR spectra of macromonomers (P1 and P2) and its precursors were recorded on a Bruker DMX-300 instrument at 300 MHz using deuterated water as solvent.

Fourier-Transform Infrared Spectroscopy (FTIR). FTIR spectra in the attenuated total reflectance (ATR) mode of the macromonomers and hydrogels were recorded using a Varian 3100 spectrometer over a wide range of 600−4000 cm^{-1} at an average of 32 scans with a resolution of ±4.0 cm^{-1}.

Gel Permeation Chromatography (GPC). The weight and the number-average molecular weights (M_w and M_n) of the prepared macromonomers P1 and P2 were determined by gel permeation chromatography apparatus (GPC, Jasco PU-2080) using a PSS Gram linear column coupled with an ETA-2020 RI detector at 23 °C. The eluent was (DMF + 0.01 M LiBr) at a flow rate of 1.0 mL/min. Calibration was carried out with PMMA150811−5 standards.

Differential Scanning Calorimetry (DSC). The water content estimations and the study of LSCT behavior of hydrogels were performed using differential scanning calorimetry (DSC) instrument (Netzsch 204) from −40 to 80 °C. The hydrogels were allowed to reach the equilibrium in deionized water at room temperature before the DSC measurements. Each hydrogel sample (~5 mg) was placed into a hermetically sealed aluminum pan and cooled to −40 °C using liquid nitrogen. The temperature was held at this temperature for 5 min to erase the thermal history and then heated at the heating rate of 3 °C/min under nitrogen atmosphere.

Swelling Ratio and Kinetics of Swelling. The swelling ratio (SR_{eq}) and equilibrium water content (EWC%) of polymer hydrogels were defined as follows

$$SR_{eq} = \frac{W_s - W_d}{W_d} \tag{1}$$

$$EWC\% = \left(\frac{W_s - W_d}{W_s}\right)100 \tag{2}$$

where W_s is the weight of the swollen hydrogels at room temperature after removing the excess surface water with a moistened filter paper and W_d is the weight of the materials dried at ambient conditions. The equilibrium values of swelling were taken after 24 h in salt solutions of 2 g/L NaCl and in deionized water (DI). In order to obtain a quantitative estimation of the swelling kinetics for the hydrogels, the weight changes of gels after immersion in deionized water were recorded at regular time intervals after water was wiped from the gels using filter paper. Water uptake (WU%) at regular time intervals was defined as follows

$$WU\% = \left(\frac{W_t - W_d}{W_s - W_d}\right)100 \tag{3}$$

where W_t is the weight of the gel at each particular time.

Determination of Water Recovery and Salt Rejection. The dewatering experiments were carried out at 50 °C for 5 min. The amount of water released was determined by taking the weight difference of the hydrogels before and after the dewatering test. Water recovery rate was derived from the weight of released water and the initial water content of the swollen hydrogels as follows

$$\text{water recovery } (\%) = \left(\frac{W_R}{W_s - W_d}\right)100 \tag{4}$$

where W_R is the weight of water released in the dewatering test.

The salt rejection was obtained by measuring the potassium concentrations of the water recovered from the hydrogels using JENCO 6230 m equipped with potassium microelectrode ISM-146 K (Lazar Research Laboratories, California, U.S.A.). The potassium concentrations were also determined by ion chromatography (Metrohm 833 Basic IC plus) using silica gel with carboxyl groups column (particle size 5 μm) at 25 °C. The eluent was (1.7 mmol/L nitric acid +0.7 mmol/L dipicolinic acid) at a flow rate of 0.9 mL/min. The chromatograph was calibrated with standard solution of Na^+ and K^+. Salt rejection was determined as follows

$$\text{salt rejection } (\%) = \left(1 - \frac{C_R}{C_0}\right)100 \tag{5}$$

where C_R and C_0 are the potassium concentrations of the water recovered from the hydrogels and that of the feed solution (2 g/L KCl), respectively.

Rheological Measurement. To investigate the mechanical properties of the fully swollen hydrogels in deionized water, frequency sweep experiments were carried out using a rheometer model MCR-300 (Anton Paar, Graz, Austria). During all measurements, a solvent trap was used to minimize evaporation. The experiments were performed in the range of ω = 0.1−100 rad/s at 20 °C with a normal force (F_N) of 3 N (within a linear range; the moduli are independent of the magnitude of imposed force) and a fixed strain of 1% using a 15 mm diameter TruGap plate corrected with a "true gap" function of the instrument.

Mesh Size Calculation of Hydrogels. Based on the rheological data and the theory of rubber elasticity,[30] the mesh size of the bulk hydrogels was estimated from the storage modulus at infinitesimal deformations. Classical theory of rubber elasticity suggests the following relationship

$$G' = n_{cl}RT \tag{6}$$

where G' is the plateau value of the storage modulus measured with frequency sweep experiment, n_{cl} is the number density of elastically effective cross-linking points (mol/m^3), R is ideal gas constant, T is the measuring temperature. Thus, at a given temperature an increase in the steady-state value of the storage modulus is related to a proportional increase in the number of network junctions. The elastic term obtained from rheological measurement is associated with the mesh size of the network from the following equation[31]

$$L = \xi = \left(\frac{1}{n_{cl}N_A}\right)^{1/3} = \left(\frac{RT}{G'N_A}\right)^{1/3} \tag{7}$$

where N_A is Avogadro's constant, assuming that the clusters are evenly dispersed and that each one is positioned in the center of a cubic-

DOI: 10.1021/acsami.5b03878
ACS Appl. Mater. Interfaces 2015, 7, 15696−15706

Table 2. Preparation and Analysis of the Macromonomers Used within This Study

polymer ID	NIPAAm (g)	AAL (g)	HESH (g)	AIBN (g)	$[S]/[M]^a$	Conv.^{b} (wt %)	$[AA]^c$ (mol %)	$M_{n,\,NMR}$ (g/mol)	$M_{n,\,GPC}$ (g/mol)	$Đ$
P1	5.65		0.316	0.084	0.055	87.3		4300	3500	1.86
P2	5.84	0.584	0.312	0.095	0.049	84.5	8	6120	5090	2.61

$^a[S]$, $[M]$ are the concentrations of chain transfer agent and monomers, respectively. ^{b}Weight of synthesized dry polymers relative to the weight of monomers. ^{c}The allyl acrylate ratio in the copolymer.

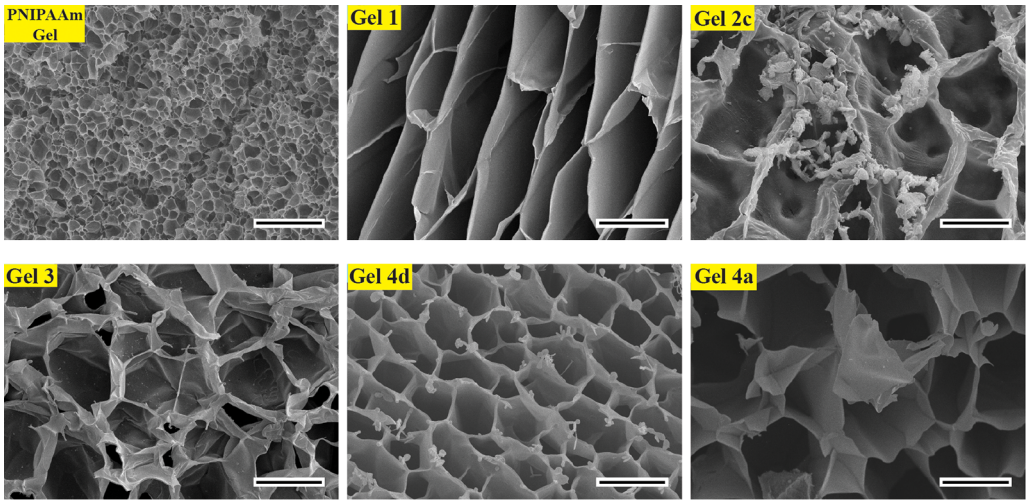

Figure 2. SEM images of the freeze-dried hydrogels with scale bars of 25 μm.

shaped volume element. Thus, the length L of a side of the cubic element can be obtained since all cubic elements combine to span the total gel volume and the total number of junctions can be deduced from eq 7 (the half length $L/2$ is the gel pore radius).

RESULTS AND DISCUSSION

Synthesis of the Thermosensitive Macromonomers. Two types of thermosensitive macromonomers, polyNIPAAm (P1) and poly(NIPAAm-*co*-AA) (P2), were prepared by radical telomerization of NIPAAm monomer and allyl alcohol (as a comonomer for P2) using HESH as a chain transfer agent followed by esterification of the hydroxyl groups. The synthesis procedure is illustrated in Scheme S1 in the Supporting Information. The resulting macromonomers were characterized by GPC and ^{1}H NMR (Table 2). Peaks of vinyl proton at 5.8–6.4 ppm were detected, indicating that polymerizable end group was introduced into the hydroxyl semitelechelic polymers (see Figure S1a, b in the Supporting Information). The M_n of the macromonomers was also determined by ^{1}H NMR from the relative integration of the methine protons of polyNIPAAm units (3.9 ppm) and the methylene proton at the end of the polyNIPAAm chains. As a result of the incorporation of the acrylate group to P2 macromonomer, the latter can act as a monomer and cross-linker. Therefore, the monomer ratio in the copolymer (P2) was calculated in order to estimate the cross-linker density for the hydrogels prepared using this macromonomer.

Preparation of the Hydrogels. It was one aim of this work to vary macromolecular architectures that have influence on the properties of thermoresponsive hydrogels. Thus, different types of polymer hydrogels were synthesized by free radical copolymerization arising from SA and three different thermally responsive components as illustrated in Scheme 1. Here, a total monomer concentration of 10 wt % was used with different cross-linker concentration in order to obtain materials with sufficient mechanical strength for the intended further characterizations. The polymerization had been performed using redox initiation at 15 °C; hence, a thermally induced microphase separation, which would affect the hydrogel structures, was considered less probable. The thermosensitive polymer was incorporated to gel 1 and gel 3 as a graft chain to form the comb-type grafted hydrogels. The backbone network of gel 1 was made up of SA and P1, while that of gel 3 was made up of SA, NIPAAm, and P1 components. Within these gels, the grafted chains had freely mobile ends, distinct from the typical network structure (gel 2 and reference PNIPAAm gel) in which both ends of chains are cross-linked and relatively immobile. It should be noted that we were not able to obtain stable gel with degree of cross-linking lower than 7 wt % for gel 1. In addition to the freely mobile ends, P2 macromonomer also provide active sites for the formation of cross-linking points to build the network. The total percentage of cross-linker used in gel 4a was calculated to be around 4 wt %, related to total monomer. The main idea for the utilization of such macromonomer was to build a two-level structure within the gel where the thermoresponsive moiety is not fragmented and at the same time is covalently connected with the polyelectrolyte, which may cause efficient mechanical forces during the volume phase transition. However, all gels were typically transparent associated with the homogeneity of the hydrogels network except for gel 4d, which was slightly turbid. This latter observation may be rationalized by the formation of cross-linker aggregates, due to the highly cross-linked hydrogel system, leading to rather compact clusters connected with shorter polymer chains, which may cause microphase separation during cross-linking copolymerization.[32,33] The polymer hydrogels were subjected to FTIR (see Figures S2a and S2b in the Supporting Information). It is noted that the infrared spectra of gels cannot be taken as the superposition of the FTIR spectra of the PNIPAAm and PSA gels. The presence of NIPAAm and SA units in the hydrogels are characterized as

DOI: 10.1021/acsami.5b03878
ACS Appl. Mater. Interfaces 2015, 7, 15696–15706

follows: broad bands in the range of 3100−3600 cm^{-1} due to the N−H stretching of amide groups, and two absorbance bands at 1643 and ∼1548 cm^{-1} attributed to the secondary amide C═O stretching (aka amide I and II bonds, respectively). The stretching vibration of C═O bonds of carboxylate groups for PSA at 1700 cm^{-1} shifted to higher frequency (1720 cm^{-1}). A C−N stretching band appears at ∼1450 cm^{-1}, confirming the presence of amide groups.

Morphology of the Hydrogels. SEM studies were carried out to reveal the morphology of the swollen freeze-dried hydrogel materials as shown in Figure 2. The micrographs show that gels exhibit a honeycomb-like structure with dense cell walls. The morphology observed, which is typical for conventional hydrogels, is not the mesh of hydrogels at their molecular level, but rather compact aggregates of the polymer chains. According to the freeze-drying process, these macropores result from the ice crystals formed within the network as a template for pore generation upon immersing the samples into liquid nitrogen.[34,35] Nevertheless, the hydrogels revealed pronounced morphological differences. The PNIPAAm gel shows smaller pore size compared to others due to incorporation of the ionic SA, which increases the water content of hydrogels. It can also be seen that the hydrogel with lower cross-linker density (gel 4a) shows much larger internal pores, and hence smaller number of pores per unit area, compared with that of higher cross-linking density (gel 4d). Large pores have been also found for gel 1, which contains graft chains without polymerizable functional groups. The small aggregates shown in gel 2c either indicate the formation of polyNIPAAm-rich domains, or may have been formed during the fracture of the frozen sample.

Swelling Properties. The water absorption of polymer hydrogels largely depends on their swelling pressure (osmotic pressure), which is the key driving force in the swelling process. According to Flory−Rehner theory,[36] the osmotic pressure within the gel is related to three major interactions: the polymer−solvent interaction π_{mix}, the entropy-elastic forces of the network π_{el}, and the contribution of the charges π_{ion}. These contributions can be expressed as a sum in the following equation.

$$\pi = \pi_{mix} + \pi_{el} + \pi_{ion} \quad (8)$$

Therefore, it is well-known that the incorporation of ionic component into hydrogel increases the equilibrium-swelling ratio (SR_{eq}); the results are shown in Figure 3 (top). Because all hydrogels (gel 1−4) contain the same amount of SA, the contribution of the charges to the osmotic pressure within all gels was estimated to be approximately constant. Thus, for particles of identical form and size, the difference in swelling ratios and the rates of water uptake should be regarded to the other contributions, which are correlated with the macromolecular architecture of the hydrogel and their composition (e.g., the degree of cross-linking). At a fixed DC, gel 4 displays the highest swelling capacity in both brine and DI indicating a looser network in the hydrogel, which can incorporate more solution. The formation of looser network can be attributed to the long spacer length between the double bond side groups (length of cross-link chain) that incorporated into P2 compared to MBAm cross-linking agent.[37] Moreover, the inherent mobile nature of the free end polyNIPAAm chains plays an important role on the swelling properties. This effect can be clearly seen for the comb-type gels 1 and 3 in DI (Figure 3, on top), where SR_{eq} are greater than that of gel 2. On the other hand, the

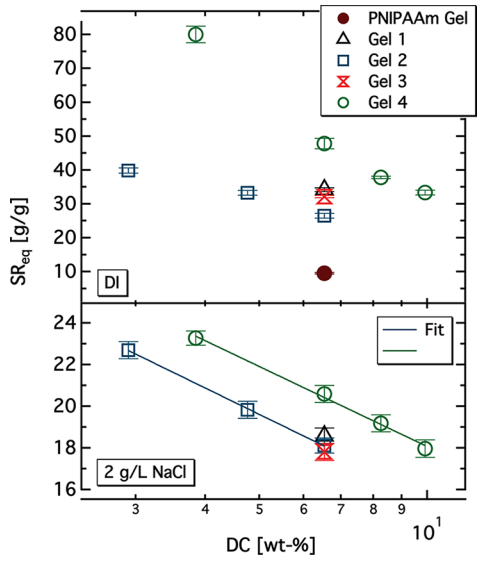

Figure 3. Equilibrium swelling ratios (SR_{eq}) of the hydrogels in deionized water (DI) (top) and in salt solution (2 g/L NaCl) (below) as a function of the cross-linking degree (DC) at room temperature (∼23 °C).

equilibrium-swelling ratio at different DC values was also investigated for gel 2 and 4 in both brine and DI. Expectedly, SR_{eq} decreases on increasing the cross-linkage, which is well-known from the literature.[38] For the measurement in brine a function of $SR_{eq} = a \log(DC) + b$ was found to present the data well, with approximately equal slope values of −12.9 for both hydrogel series (Figure 3, below). This indicates that the contribution of charges in the osmotic pressure is the same resulting in equal salt depletion.

The dynamic of swelling process have been also determined for a few hydrogel samples by measuring the water uptake (WU) at different times. The results are shown in Figure 4 and the kinetic was found to be varying with the type of hydrogels. However, to extract the rate constants of the water absorption, a sigmoid function was fitted to the data.

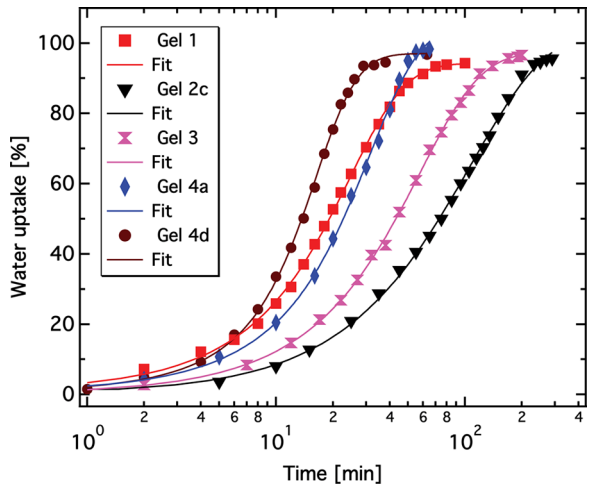

Figure 4. Plots of water uptake as a function of swelling time in deionized water (DI) at room temperature (∼23 °C). The sample form and size were constant for all samples (cylinder, 5 mm in diameter and 2 mm in thickness).

DOI: 10.1021/acsami.5b03878
ACS Appl. Mater. Interfaces 2015, 7, 15696−15706

$$WU(t) = WU_0 + \left(\frac{WU_{max}}{1 + e^{\frac{t_{half} - t}{\tau}}} \right) \quad (9)$$

where $WU(t)$, WU_0, and WU_{max} are the percentage of water uptake at time t, ground, and maximum, respectively. t_{half} is the first derivative maximum of the function or the inflection point, and τ is the rate constant of the water uptake described by the slope of curve. The rate constants were determined to be 6, 13, 15, 35, and 89 min for gel 4d, 1, 4a, 3, and 2, respectively. This can be attributed to the fact that the distance between the pores in gel 4d is smaller, and then water molecules can diffuse in faster compared to gel 4a. The mobility of the grafted chains in gel 1 and 4, in addition to the flexibility of the cross-linking chains for gel 4, also allowed them to be structurally separated from the backbone of the cross-linked network, permitting fast hydration compared to gel 2 and 3.

Rheological Investigation and Network Structure. The mechanical properties of the fully swollen hydrogels in deionized water were characterized by recording the influence of frequency on elastic modulus (G') and loss modulus (G'') (Figure 3S in the Supporting Information). All gels exhibit a plateau or frequency independent response of storage modulus in the range from 0.1 to 100 rad/s, which reveals that this gel had indeed soft rubbery-like behavior (ideal gel). A notable exception is gel 4a (gel without MBAm cross-linker) that presented gradual rise in G' not only because of the free chain ends and the flexibility of the cross-linking chains but also because of the low cross-linker density of the network. However, the modulus in the rubbery range is related to the change in entropy. Therefore, the change in stiffness or toughness of the network can be correlated with the cross-linker density of gels. Figure 5 shows that, there is indeed a

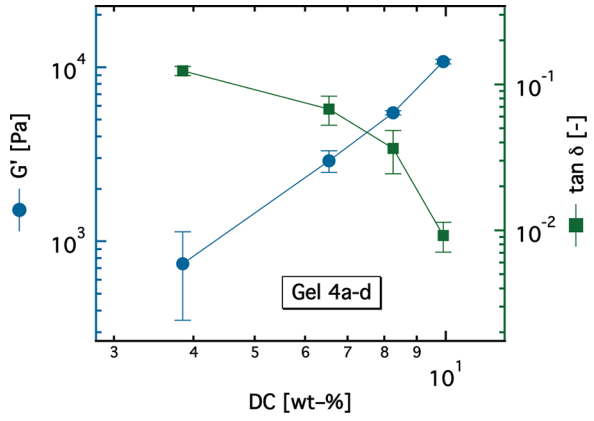

Figure 5. Storage modulus (G') and loss tangent (tan δ) as a function of cross-linking degree (DC) for gel 4.

linear increase of G' with DC for gel 4. More cross-links introduce shorter polymer chain segments that exert a higher elastic force. As we stated in the swelling properties presented above, gels with fixed DC and different macromolecular architecture led to different SR_{eq}. In this context, a correlation between storage modulus and swelling ratio at equilibrium was well investigated as shown in Figure 6. Gels with more water per unit volume exhibit a reduction of the elastic modulus. An increase in the viscous part for gel 4b, which shows the highest swelling ratio, was also observed.

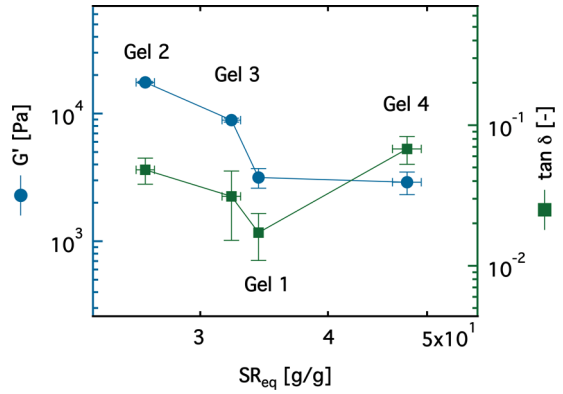

Figure 6. Storage modulus (G') and loss tangent (tan δ) as a function of the equilibrium-swelling ratio of gels at a fixed cross-linking degree (DC) of 7 wt %.

To describe the microstructure of hydrogels, their mesh length was estimated from rheological data using eq 7 and the obtained values were correlated with SR_{eq} data. A linear relationship as shown in Figure 7 was obtained.

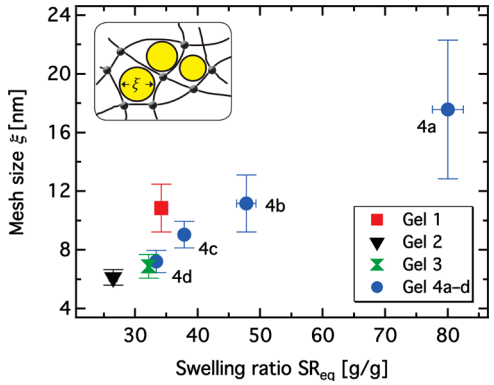

Figure 7. Correlation of the mesh sizes estimated from rheological data with the swelling ratio at equilibrium of hydrogels in deionized water (DI).

The state of absorbed water could also provide valuable information about the porosity inside the hydrogels and thus the major swelling/deswelling mechanism. According to the thermodynamic properties, any swollen hydrogel contains three different states of water in its network:[39] (1) freezable free water, which exists without any hydrogen bonding with the polymer chains and behaves similarly with pure water as far as freezing and melting is concerned; (2) freezable bound water, which exhibits weak interactions with polymeric chains within the network of hydrogels and freezes/melts at temperature shifted with respect to that of free water; and (3) nonfreezable bound water, which binds to polymer chains through hydrogen bounding and does not show any endothermic peak within the normal temperature range associated with pure water. DSC thermograms of the fully swollen hydrogels in DI (Figure 8a) display that the melting of water in all samples starts at temperature lower than that of pure water (dashed line). Generally, for all studied gels the endothermic peaks are broad and structured. For some samples, two well-defined submaxima can be observed, demonstrating the existence of two types of freezable water as we discussed above.

DOI: 10.1021/acsami.5b03878
ACS Appl. Mater. Interfaces 2015, 7, 15696−15706

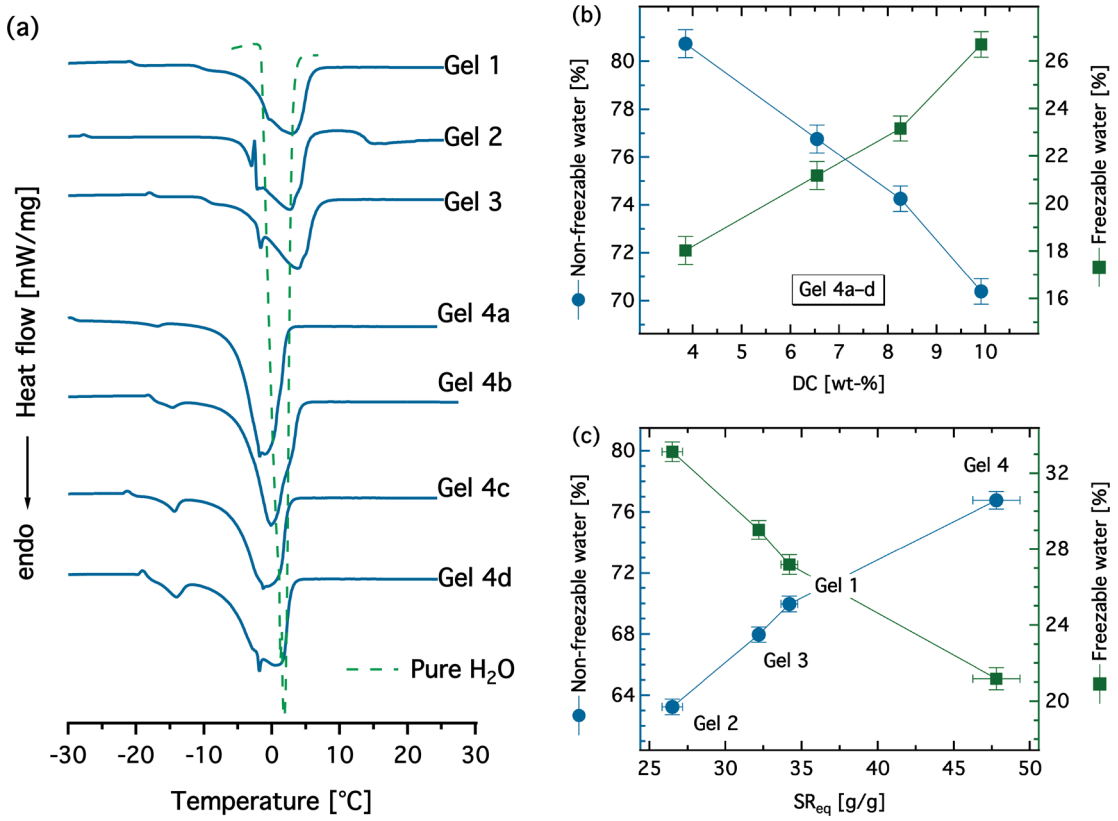

Figure 8. (a) DSC thermograms for the studied hydrogels, and (b, c) the estimated nonfreezable and freezable water content as a function of (b) cross-linking degree (DC) and (c) swelling ratio at equilibrium at a fixed (DC) of 7 wt %.

The presence of nonfreezable water can be estimated by following a standard procedure described by Mansor and Malcolm.[40] The amount of unbound water was calculated with the assumption that the heat of fusion of unbound water in the hydrogel was the same as that for ice applying the following equation

$$W_b(\%) = W_c - (W_f + W_{fb}) = W_c - \left(\frac{Q_{endo}}{Q_{pure}}\right) \times 100 \quad (10)$$

where W_c, W_b, W_f, and W_{fb} are the equilibrium water content (%) (EWC), the amount of nonfreezable bound water (%), the amount of freezable free water (%), and the amount of freezable bound water (%), respectively, whereas Q_{endo} is defined as the heat of fusion of freezable water (freezable free water and freezable bound water) within the hydrogels and Q_{pure} is the heat of fusion of ice (340.1 J/g).

The influence of the cross-linking degree of gel 4 on nonfreezable water content was investigated as shown in Figure 8b. The amount of nonfreezable water is decreasing with increasing the number of cross-links and this is to be expected. In contrast, the amount of nonfreezable water is increasing as the SR_{eq} increase at a fixed DC for gels with different macromolecular architecture as shown in Figure 8c.

Dewatering Study and Salt Rejection. The dewatering process (see Figure 9) was achieved in this study via thermal heating, yielding release of water. The percentage of water recovery for swollen polymer hydrogels after 60 min dewatering process for both bulk and powder gels (Figure 10c) were determined under relatively low temperature conditions (50 °C) using eq 4. First, we confirm the principle of the desalination idea by examining the water release from the swollen PNIPAAm gel at the same condition. It exhibits a water recovery of around 70% (data not shown, see Figure 9 on top), and this value is comparable to that reported by other work groups.[23,41]

Figure 11a, c shows the percentage of water recovery of the swollen bulk gels (on top) and powder gels (down) after equilibrium loading in brine solutions of 2 g/L NaCl. It should be noted that the values of swelling at equilibrium using gel as powder were higher than that of bulk gel. The bulk gels as well as the powder gels display low thermally responsive water recovery with percentage recoveries being less than 10% even with ultrapure water (see Figure S4 in the Supporting Information). The influence of cross-linking degree on the water recovery was also investigated for gel 2 and 4 (Figure 11b, d). The water recovery is slightly increasing as the DC increases for both bulk and powder gels. It was observed, that the majority of the water loss for the bulk gels was in the vapor state (because the weight difference of the hydrogels before and after the dewatering process was lower than the weight of recovered water). For further support, the loss of water in the vapor state was also tested using a plug (made of tea bag) and filled with superabsorber (Figure 10b). The recovered water in the form of vapor was thus calculated from the weight difference of the plug before and after 60 min dewatering process and was found to be in the range of 20−30% (see Figure S5 in the Supporting Information). This indicates that the release-associated mechanism is not completely related to stimulus-induced mechanical dewatering as aimed at in the introduction.

DOI: 10.1021/acsami.5b03878
ACS Appl. Mater. Interfaces 2015, 7, 15696−15706

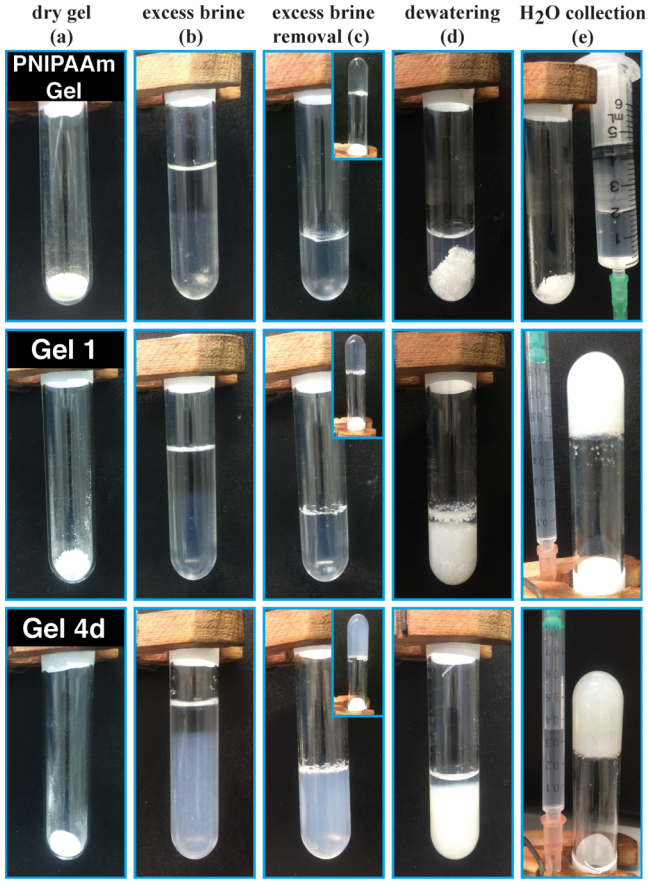

Figure 9. Photographs represent the steps of the desalination process using powder gels, where (a) is the gel in dry state, (b) swelling of the gels in an excess salt water, (c) removal of the excess solution, (d) dewatering of the gels by thermal heating for 60 min at 50 °C, (e) collection of the recovered water.

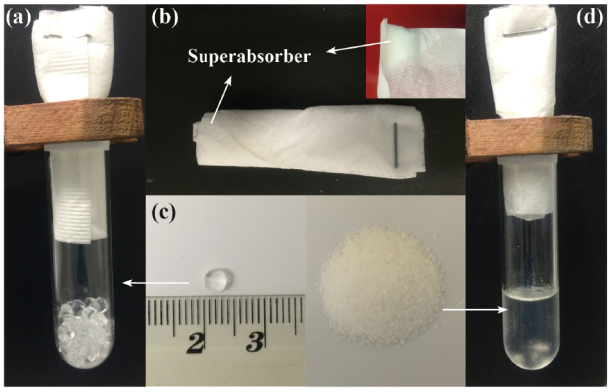

Figure 10. Photograph of the test used to determine the water loss via the vapor phase. (a) Gel from bulk samples (d), gel from powder samples. (b) Plug prepared to adsorb the water from the vapor phase and (c) images of the thermoresponsive gels used in (a) and (d).

In this context, the hydrogel was also subjected to differential scanning calorimetry (DSC), in order to explore the phase transition behavior. Unlike PNIPAAm gel, none of the gels did display endothermic peak representing the phase transition (LCST) in the range between 25 and 80 °C, although the transparent gel 1 became opaque just after the temperature increase above the LCST of polyNIPAAm indicating formation of a heterogeneous structure. It seems that only the comb-like grafted polyNIPAAm (P1) chains caused a cloud point, while the cross-linked SA network remained unchanged. On the other hand, the low percentage of water recovery for gel 2 as well as gel 3 is related to the division of the polyNIPAAm network into multiple short segments and thus the hydrophobic aggregation force decreased during the dewatering or shrinking course. It was reported that the LCST will increase dramatically and even disappears once many SA segments were randomly introduced to the hydrogel (SA unit fraction is higher than 1.3 wt %).[42] Therefore, gel 2 and 3 kept their transparency during the dewatering due to the small size of hydrophobic aggregates compared with the wavelength of visible light. To avoid the fragmentation of the linear polyNIPAAm chains, we designed gels 4, which may show, in our opinion, more driving force to squeeze the water out of the hydrogel. Unfortunately, the water recovery was not as we expected, although gel 4 showed novel behavior related to kinetics study of swelling. The lack of the thermally induced dewatering mechanism may be rationalized by the following hypothetical reasons: (1) strong molecular interaction between water and polymer chains (hydrogen bonds); (2) slow dehydration, which is related to the balance of forces attributing to the hydrophobicity and hydrophilicity, resulting in weak hydrophobic aggregation of the entire hydrogels. However, less carboxylate content will definitely increase the overall driving force for such a process, resulting in higher water recovery rate, but in contrast the swelling capacity and the possibility of salt depletion will be also reduced.

The salt rejection was determined for a few hydrogel samples by measuring the ion concentrations of the water released after dewatering at 50 °C and in feed solution using potassium microelectrode. For this purpose we used a salt solution of 2 g/L KCl to prevent any interference with sodium ions located within the gels. Identical swelling ratios and water recovery rates were observed for the hydrogels upon using brine of KCl solutions. For verification, comparison was also made with the salt rejection measured by ion chromatography as shown in Figure 12. The data obtained from IC show a slightly higher salt rejection for gel 1, 3, and 4d as compared with the other method, which might be due to the interference from the sodium ions. Nevertheless, gel 1 shows the highest salt rejection of 23% in one cycle, while the salt rejection for gel 2 was the lowest. We attribute this to the graft structure of gel 1, which maintains the large content of ions in the hydrogel backbone. No major difference in the salt rejection between the bulk and the powder gels were found.

CONCLUSION

In the present study, materials for an alternative method for the desalination of brackish water by swelling and thermal deswelling hydrogels are presented. We have successfully prepared a series of polymeric networks varying the structural type of the thermoresponsive comonomer based on NIPAAm using free radical copolymerization technique. Unlike the dewatering behavior, the swelling kinetic was found to be strongly dependent on the macromolecular architecture of the hydrogels and their composition. The rheological behavior of hydrogels and the DSC measurements also supported this effect. Preferable samples are powders with a high DC. Gel 1 displayed the maximum amount of recovered water (~10%) using 2 g/L salt solution as a feed, from which salt concentration could be reduced by ~23% in one cycle. Today, all developments in desalination technologies are

DOI: 10.1021/acsami.5b03878
ACS Appl. Mater. Interfaces 2015, 7, 15696−15706

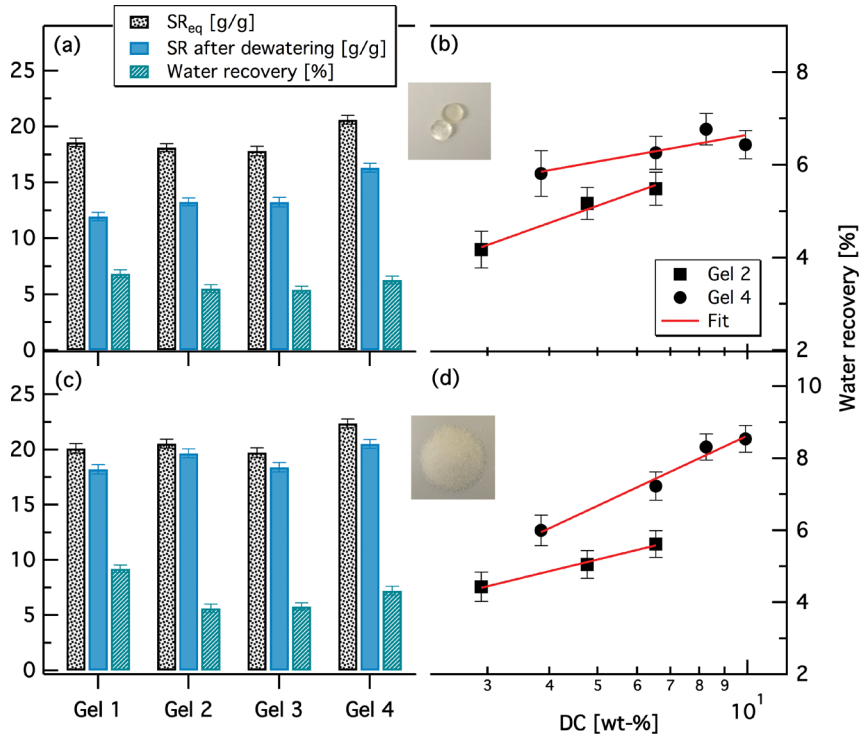

Figure 11. Percentage of water recovery from fully swollen gels with 7 wt % DC after 60 min dewatering process at 50 °C: (a) bulk and (c) powder gels; (b, d) influence of DC on the water recovery for gels 2 and 4. Gels were swollen in a salt solution of 2 g/L NaCl.

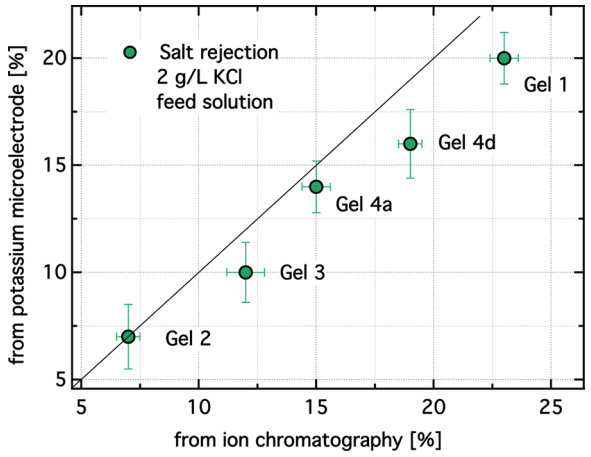

Figure 12. Salt rejection upon swelling/deswelling process with 2 g/L KCl as feed saline water in one cycle using bulk gels.

aimed at reducing energy consumption and cost, in addition to minimize environmental impacts. Available evidence indicates that significant amounts of brackish water exist as aquifers, which is used even without treatment, especially in the poor communities. Therefore, it is believed that this work holds promise for desalting brackish water with more optimized hydrogel structures to follow. Subsequent work will focus on the improvement of the water recovery rate by introducing the ionic moieties as pendent chains in the polyNIPAAm network to keep the strong hydrophobic backbone aggregation using another polymerization technique.

■ ASSOCIATED CONTENT

Supporting Information

Synthesis procedure of the thermosensitive macromonomers P1 and P2, partial ^{1}H NMR spectra of the thermosensitive semitelechelic polymers and the macromonomers P1 and P2, FTIR spectra of hydrogels, plots of storage modulus (G'), loss modulus (G''), and loss tangent (tan δ) as a function of angular frequency (ω), and the percentage of water recovery in in both liquid and vapor states. The Supporting Information is available free of charge on the ACS Publications website at DOI: 10.1021/acsami.5b03878.

■ AUTHOR INFORMATION

Corresponding Author

*E-mail: Jochen.gutmann@uni-due.de.

Notes

The authors declare no competing financial interest.

■ ACKNOWLEDGMENTS

We express thanks for the financial support by Atomic Energy Commission of Syria (AECS). The authors also thank Mr. T. Urbainczyk, Universität Duisburg-Essen, for his helpful support.

■ REFERENCES

(1) *Vital Water Graphics, An Overview of the State of the World'S Fresh and Marine Waters*, 2nd ed.; UNEP: Nairobi, Kenya, 2008.

(2) *World Water Assessment Programme (WWAP): The United Nations World Water Development Report 4: Managing Water under Uncertainty and Risk*; UNESCO Publishing: Paris, 2012.

(3) Shannon, M. A.; Bohn, P. W.; Elimelech, M.; Georgiadis, J. G.; Marinas, B. J.; Mayes, A. M. Science and Technology for Water Purification in the Coming Decades. *Nature* **2008**, *452*, 301−310.

DOI: 10.1021/acsami.5b03878
ACS Appl. Mater. Interfaces 2015, 7, 15696−15706

(4) Geise, G. M.; Lee, H. S.; Miller, D. J.; Freeman, B. D.; Mcgrath, J. E.; Paul, D. R. Water Purification by Membranes: The Role of Polymer Science. *J. Polym. Sci., Part B: Polym. Phys.* **2010**, *48*, 1685−1718.
(5) Fritzmann, C.; Lowenberg, J.; Wintgens, T.; Melin, T. State-of-the-art of Reverse Osmosis Desalination. *Desalination* **2007**, *216*, 1−76.
(6) Wichterle, O.; Lím, D. Hydrophilic Gels for Biological Use. *Nature* **1960**, *185*, 117−118.
(7) Flory, P. J. *Principles of Polymer Chemistry*, 1st ed.; Cornell University Press: Ithaca, NY, 1953.
(8) Mark, J. E.; Erman, B. *Rubberlike Elasticity*, 1st ed.; Wiley−Interscience: New York, 1988.
(9) Wack, H.; Ulbricht, M. Effect of Synthesis Composition on the Swelling Pressure of Polymeric Hydrogels. *Polymer* **2009**, *50*, 2075−2080.
(10) Höpfner, J.; Klein, C.; Wilhelm, M. A Novel Approach for the Desalination of Seawater by Means of Reusable Poly(acrylic acid) Hydrogels and Mechanical Force. *Macromol. Rapid Commun.* **2010**, *31*, 1337−1342.
(11) Shibayama, M.; Tanaka, T. *Responsive Gels: Vol. Transitions I (Advances in Polymer Science)*; Springer, Berlin, 1993; Vol. *109*, p 1−62.
(12) Yang, Q.; Adrus, N.; Tomicki, F.; Ulbricht, M. Composites of Functional Polymeric Hydrogels and Porous Membranes. *J. Mater. Chem.* **2011**, *21*, 2783−2811.
(13) Tanaka, T. Collapse of Gels and the Critical Endpoint. *Phys. Rev. Lett.* **1978**, *40*, 820−823.
(14) Horikawa, Y.; Tanaka, T.; Matsuo, E. S. Volume Phase Transition in a Nonionic Gel. *J. Chem. Phys.* **1984**, *81*, 6379−6380.
(15) Schild, G. H. Poly(*N*-isopropylacrylamide): Experiment, Theory, and Application. *Prog. Polym. Sci.* **1992**, *17*, 163−249.
(16) Rzaev, Z. M. O.; Dincer, S.; Piskin, E. Functional Copolymers of *N*-isopropylacrylamide for Bioengineering Applications. *Prog. Polym. Sci.* **2007**, *32*, 534−595.
(17) Bloch, H. S. Removal of water from aqueous solutions. U.S. Patent 3 234 125, Feb. 8, 1966.
(18) Anderson, R. E.; Jones, G. D. Desalination of water with thermally reversible water-swellable resins. U.S. Patent 3 438 893, Apr. 15, 1969.
(19) Hass, H. C. Hass solvent extraction process. U.S. Patent 3 451 926, Jun 24, 1969.
(20) Fletcher, E. M. Water removal from water-containing media. U.S. Patent 3 441 501, Apr. 29, 1969.
(21) Glavis, F. J.; Clemens, D. H. Desalination process. U.S. Patent 3 753 898, Aug. 21, 1973.
(22) Blair, E. A. Desalination Process. U.S. Patent 5 354,835, Oct. 11, 1994.
(23) Li, D.; Zhang, X. Y.; Yao, J. F.; Simon, G. P.; Wang, H Stimuli-responsive Polymer Hydrogels as a New Class of Draw Agent for Forward Osmosis Desalination. *Chem. Commun.* **2011**, *47*, 1710−1712.
(24) Li, D.; Zhang, X. Y.; Yao, J. F.; Zeng, Y.; Simon, G. P.; Wang, H. Composite Polymer Hydrogels as Draw Agents in Forward Osmosis and Solar Dewatering. *Soft Matter* **2011**, *7*, 10048−10056.
(25) Zeng, Y.; Qiu, L.; Wang, K.; Yao, J.; Li, D.; Simon, G. P.; Wang, R.; Wang, H. Significantly Enhanced Water Flux in Forward Osmosis Desalination with Polymer-graphene Composite Hydrogels as a Draw Agent. *RSC Adv.* **2013**, *3*, 887−894.
(26) Razmjou, A.; Barati, M. R.; Simon, G. P.; Suzuki, K.; Wang, H. Fast Deswelling of Nanocomposite Polymer Hydrogels via Magnetic Field-induced Heating for Emerging FO Desalination. *Environ. Sci. Technol.* **2013**, *47*, 6297−6305.
(27) Yoshida, R.; Uchida, K.; Sakal, K.; Kiruchi, A.; Sakurai, Y.; Okano, T. Comb-type Grafted Hydrogels with Rapid Deswelling Response to temperature Changes. *Nature* **1995**, *374*, 240−242.
(28) Kaneko, Y.; Sakai, K.; Kikuchi, A.; Yoshida, R.; Sakurai, Y.; Okano, T. Influence of Freely Mobile Grafted Chain Length on Dynamic Properties of Comb-type Grafted Poly(*N*-isopropylacrylamide) Hydrogels. *Macromolecules* **1995**, *28*, 7717−7723.
(29) Chen, G.; Hoffman, A. S. Graft Copolymers that Exhibit Temperature-induced Phase Transitions over a Wide Range of pH. *Nature* **1995**, *373*, 49−52.
(30) Canal, T.; Peppas, N. A. Correlation between Mesh Size and Equilibrium Degree of Swelling of Polymeric Networks. *J. Biomed. Mater. Res.* **1989**, *23*, 1183−1193.
(31) Wang, J.; Ugaz, V. M. Using in situ Rheology to Characterize the Microstructure in Photopolymerized Polyacrylamide Gels for DNA Electrophoresis. *Electrophoresis* **2006**, *27*, 3349−3358.
(32) Okay, O.; Oppermann, W. Polyacrylamide-clay Nanocomposite Hydrogels: Rheological and Light Scattering Characterization. *Macromolecules* **2007**, *40*, 3378−3387.
(33) Cohen, Y.; Ramon, O.; Kopelman, I. J.; Mizrahi, S. Characterization of Inhomogeneous Polyacrylamide Hydrogels. *J. Polym. Sci., Part B: Polym. Phys.* **1992**, *30*, 1055−1067.
(34) Kang, H. W.; Tabata, Y.; Ikada, Y. Fabrication of Porous Gelatin Scaffolds for Tissue Engineering. *Biomaterials* **1999**, *20*, 1339−1344.
(35) Zhang, X.-Z.; Yang, Y.-Y.; Chung, T.-S. The Influence of Cold Treatment on Properties of Temperature-sensitive Poly(*N*-isopropylacrylamide) Hydrogels. *J. Colloid Interface Sci.* **2002**, *246*, 105−111.
(36) Flory, J. P.; Rehner, J. Statistical Mechanism of Cross-linked Polymer Networks. I. Rubberlike Elasticity. *J. Chem. Phys.* **1943**, *11*, 512−520.
(37) Mabilleau, G.; Stancu, I. C.; Honoré, T.; Legeay, G.; Cincu, C.; Baslé, M. F.; Chappard, D. Effects of the Length of Crosslink Chain on Poly(2-hydroxyethyl methacrylate) (pHEMA) Swelling and Biomechanical Properties. *J. Biomed. Mater. Res., Part A* **2006**, *77A*, 35−42.
(38) Okajima, T.; Harada, I.; Nishio, K.; Hirotsu, S. Kinetics of Volume Phase Transition in Poly(*N*-isopropylacrylamide) Gels. *J. Chem. Phys.* **2002**, *116*, 9068−9077.
(39) Hoffman, A. S. Hydrogels for Biomedical Applications. *Adv. Drug. Delivery Rev.* **2002**, *43*, 3−12.
(40) Mansor, B. A.; Huglin, M. B. DSC Studies on States of Water in Crosslinked Poly(methyl methacrylate-*co*-*n*-vinyl-2-pyrrolidone) Hydrogels. *Polym. Int.* **1994**, *33*, 273−277.
(41) Cai, Y.; Shen, W.; Loo, S. L.; Krantz, W. B.; Wang, R.; Fane, A. G.; Hu, X. Towards Temperature Driven Forward Osmosis Desalination Using Semi-IPN Hydrogels as Reversible Draw Agents. *Water Res.* **2013**, *47*, 3773−3781.
(42) Zhang, X.-Z.; Xu, X.-D.; Cheng, S.-X.; Zhuo, R.-X. Strategies to Improve the Response Rate of Thermosensitive PNIPAAm Hydrogels. *Soft Matter* **2008**, *4*, 385−391.

DOI: 10.1021/acsami.5b03878
ACS Appl. Mater. Interfaces 2015, 7, 15696−15706